Final Report: W911NF-21-2-0080 PI: John Eaton, Stanford University

List of Figures

Statement of Problem Studied

Contaminant plumes produced by fires, explosions, accidental releases, or terrorist acts in urban settings can be deadly to large numbers of people. In particular, first responders or combatants in urban arenas of conflict can be exposed to the devastating initial conditions but also to the hazards associated with lingering contaminants that are slow to disperse. The dispersion of chemicals, particles, or biological agents in these plumes is typically dominated by turbulent transport as the normally highly turbulent plume interacts with the turbulent atmospheric boundary layer in the context of an extremely complex urban environment. Three-dimensional measurements are critical to understand the physical mechanisms behind plume dispersion and to test and validate analytical and computational models for predicting velocities and contaminant concentrations. 3D mean velocity and concentration measurements throughout 3D printed replicas of real world urban environments can be acquired using Magnetic Resonance Velocimetry (MRV) and Magnetic Resonance Concentration (MRC) methods. The MRV and MRC scanning sequences detect the motion of hydrogen protons bound in water so experiments are done in fully turbulent water channels with scaled but realistic geometries. The experiments are conducted at Reynolds numbers orders of magnitude below full scale, but extensive experience has shown that both mean transport and turbulent dispersion are very weakly affected by Reynolds number in complex topography as long as the flow is fully turbulent. A series of MRI-based experiments were conducted with a United States Military Academy (USMA) cadet team during the 2019-2020 academic year (Chung

REPORT DOCUMENTATION PAGE

Form Approved
OMB No. 0704-0188

PLEASE DO NOT RETURN YOUR FORM TO THE ABOVE ADDRESS.

1. REPORT DATE *(DD-MM-YYYY)*	2. REPORT TYPE	3. DATES COVERED *(From - To)*
14-06-2022	Final	March 2021- July 2022

4. TITLE AND SUBTITLE

Investigation of Transient Contaminant Dispersion in Mock Urban Canopies

5a. CONTRACT NUMBER

W911NF-21-2-0080

5b. GRANT NUMBER

5c. PROGRAM ELEMENT NUMBER

6. AUTHOR(S)

Elkins, Christopher
Banko, Andrew
Eaton, John

5d. PROJECT NUMBER

5e. TASK NUMBER

5f. WORK UNIT NUMBER

7. PERFORMING ORGANIZATION NAME(S) AND ADDRESS(ES)

LELAND STANFORD JUNIOR UNIVERSITY, THE
STANFORD UNIVERSITY
450 JANE STANFORD WAY
STANFORD CA 94305-2004

8. PERFORMING ORGANIZATION REPORT NUMBER

9. SPONSORING/MONITORING AGENCY NAME(S) AND ADDRESS(ES)

US ARMY ACC-APG-RTP W911NF
800 PARK OFFICE DRIVE, SUITE 4229
RESEARCH TRIANGLE PARK NC 27709

10. SPONSOR/MONITOR'S ACRONYM(S)

11. SPONSOR/MONITOR'S REPORT NUMBER(S)

12. DISTRIBUTION/AVAILABILITY STATEMENT

A-Unlimited

13. SUPPLEMENTARY NOTES

14. ABSTRACT

Contaminant plumes produced by fires, explosions, accidental releases, or terrorist acts in urban settings can be deadly to large numbers of people. The dispersion of chemicals, particles, or biological agents in these plumes is typically dominated by turbulent transport as the highly turbulent plume interacts with the turbulent atmospheric boundary layer in the context of a complex urban environment. Three-dimensional measurements are critical to understand the physical mechanisms behind plume dispersion and to test and validate analytical and computational models for predicting velocities and contaminant concentrations. A series of MRI-based experiments were conducted for a transient plume in a scale model of Oklahoma City circa 2003. These experiments acquired volumetric, phase-averaged velocity and concentration data. At each point, the measurements show both the amplitude of concentration oscillations and phase lag relative to the source oscillations. Thus, the data are ideally suited for validating models of transient releases. This program supported the analysis of these data to understand basic dispersion phenomena as well as develop advanced data analysis tools such as those based on discrete Green's functions and the Finite Time Lyapunov Exponent (FTLE).

15. SUBJECT TERMS

Magnetic Resonance Velocimetry, Magnetic Resonance Concentration, Contaminant Dispersion, Transient Plume, Urban Environment, Scalar Flux, Finite Time Lyapunov Exponent Field

16. SECURITY CLASSIFICATION OF:			17. LIMITATION OF ABSTRACT	18. NUMBER OF PAGES	19a. NAME OF RESPONSIBLE PERSON
a. REPORT	b. ABSTRACT	c. THIS PAGE			John K. Eaton
U	U	U		9	19b. TELEPHONE NUMBER *(Include area code)* 650 804-9279

et al (2020)) for a transient plume in a 1:2206 scale model of Oklahoma City circa 2003. These experiments acquired volumetric, phase-averaged velocity and concentration data. At each point, the measurements show both the amplitude of concentration oscillations and phase lag relative to the source oscillations. Thus, the data are ideally suited for validating models of transient releases. The results from the experiments and preliminary analysis have been compiled for distribution to the appropriate agencies for future CFD model development and policy making, and the first of several journal articles based on the data has been published. This program supported the analysis of these data to understand basic dispersion phenomena as well as develop advanced data analysis tools such as those based on discrete Green's functions and the Finite Time Lyapunov Exponent (FTLE) field. These tools have potential for predicting contaminant cloud dispersion from transient plumes for a wide variety of environments.

Summary of Most Important Results

Details of the experiment and preliminary analysis can be found in Chung et al 2020. More comprehensive details and analysis including the control volume analysis completed under this project are found in Homan et al. 2021. Briefly, a passive scalar was injected at street level in a scaled model of Oklahoma City, circa 2003 (see Figure 1). The injection used a 40% duty cycle square waveform with frequency of 1 Hz to create a transient plume upstream of several buildings as shown. Magnetic Resonance Velocimetry and Concentration (MRV and MRC) methods were used to measure phase-averaged velocity and concentration for 12 intervals during the release cycle. Figure 2 helps visualize the evolution of the phase-averaged scalar plume as it advects downstream, interacts with the urban geometry, and is dispersed by turbulence.

As part of the advanced analysis supported by this project, a time-dependent control volume analysis was conducted for two regions of the geometry highlighted by the red volumes shown in Figure 3. The analysis attempts to calculate the turbulent scalar flux from imbalances between the net scalar flux (flux in minus flux out) and storage terms both of which can be calculated using the phase-averaged velocity and concentration terms.

The net flux and the transient storage term are balanced for the western control volume (subfigure 2 of Fig. 3) throughout the entire cycle to within the experimental uncertainty. The largest potential discrepancy is near $t/T = 1$ where the net flux has a sharply peaked minimum. However, the temporal resolution combined with the finite difference approximation of the time derivative is expected to result in an underestimation of the storage term magnitude. Overall, the turbulent fluxes are anticipated to be small for the western control volume because this flow path is unobstructed by buildings and most of the transport occurs through the north and south faces of the control volume.

Differences between the net flux and storage time series are observed for the intersection control volume in subfigure 1 near $t/T = 0.4$ and $t/T = 1$. These points serve as tentative evidence for the importance of turbulent scalar flux to the contaminant transport within the intersection at specific times during the transient release. Time $t/T = 0.4$ indicates a net turbulent flux of contaminant into the control volume and is associated with the initial arrival of the plume, as indicated by the rise in the advective flux into the intersection. Time $t/T = 1$ indicates a net turbulent flux of

contaminant out of the control volume and coincides with the greatest rate of decrease of contaminant within the intersection. In this case, it is hypothesized that the boundary between clean flow and contaminated flow is unsteady, leading to turbulent fluctuations in contaminant across the northern control volume face. This time dependence of the imbalance between the mean scalar flux and storage term suggests that the importance of the turbulent scalar flux varies as the plume disperses through the control volume.

Another advanced analysis tool we developed is based on the discrete Green's function (DGF) which is an impulse response function that can be found using a reverse optimization procedure. For this experiment with a transient contaminant plume advecting with the flow, the DGF represents the impulse response of the time dependent three-dimensional concentration field to an injection of contaminant in the flow geometry. The DGF allows one to generalize the 40% duty-cycle injection to arbitrary injection schemes for that source location and a fixed mean flow field (i.e. the same wind direction). Statistics such as plume residence time and maximum exposure can be assessed from the DGF. If multiple sources are present, then the DGFs from each source can be linearly combined to infer the concentration fields from simultaneous releases. The DGF also provides access to the steady-state concentration field from a continuous release. Therefore, the DGF allows one or several MRC experiments to generalize to a multitude of new scenarios making it useful for emergency planning and comparing MRC data to field or wind tunnel measurements when the release profiles cannot be precisely matched across experiments.

Figure 4 shows examples of calculations that can be performed with the DGF. The local total exposure time can be found by integrating the DGF over the cycle period, and the local peak exposure is the maximum value of the DGF. It is interesting to compare the two plots and note regions where peak exposure is high but total exposure is low as seen in some regions around the injector and vice-versa in a couple of the cross streets in between the buildings downstream. Because the DGF is generalizable, similar calculations could be generated for completely different release waveforms.

The final advanced analysis tool developed is based on identifying transport boundaries using the finite time Lyapunov exponent (FTLE) field computed from the 3D experimental mean velocity data. The MRI measurements indicate that passive scalar dispersion within the urban canopy is governed by a combination of turbulent dispersion and mechanical dispersion due to the complex 3D mean flow around buildings. Complex flow topology produced by the 3D urban geometry, including separation bubbles and convergence zones, can enhance the mechanical dispersion beyond the simple geometric footprint of the buildings. Figure 5(a) provides an example of the impact of flow topology on the lateral dispersion of a plume in the Oklahoma City geometry. The in-plane vector field suggests that topological surfaces of the mean flow field separate clean and contaminated flow, and therefore contribute to the mechanical dispersion. We term these surfaces transport boundaries since the mean scalar flux perpendicular to the surface appears small.

The 3D nature of MRI data allows the transport boundaries to be quantitatively extracted from the flow field. Transport boundaries are defined as ridges of the FTLE field which identify

hyperbolic manifolds corresponding to exponentially separating or repelling fluid trajectories. This definition agrees with the qualitative observations described above, because the mean flux perpendicular to an FTLE ridge is small. The FTLE field corresponding to exponentially converging trajectories is shown in Figure 5 which shows contours of the FTLE field (b) and ridges shown in gray (a). Note the close correspondence between the ridges, the separatrices demarcating convergence zones and separation bubbles in the vector field, and the boundaries between clean and contaminated flow. Additional analysis has been performed to quantify the correlation between transport boundaries and strong spatial gradients in the scalar field. The MRI data also provides unique insight into the 3D structure of these surfaces, and therefore their effect on both lateral and vertical dispersion.

We anticipate that transport boundaries will be a useful tool for validating computational fluid dynamics models used for predicting scalar dispersion in urban areas. This is because they are strongly correlated with mechanical dispersion and they reduce the dimensionality of large, 3D datasets while retaining important dynamical information.

Several advanced analysis techniques were applied to the three-dimensional MRV/MRC data that have never been applied before. All of them show great promise for extracting important information about this particular transient plume flow field. More importantly, the techniques are generalizable to other three-dimensional datasets and capable of producing estimates for turbulent scalar flux, statistics about plume dispersion for arbitrary transient releases, and identification of mechanical dispersion transport boundaries. These are all quantities that can help better utilize 3D data for comparing and validating CFD and create better reduced order models to be used by first responders and other health and safety officials.

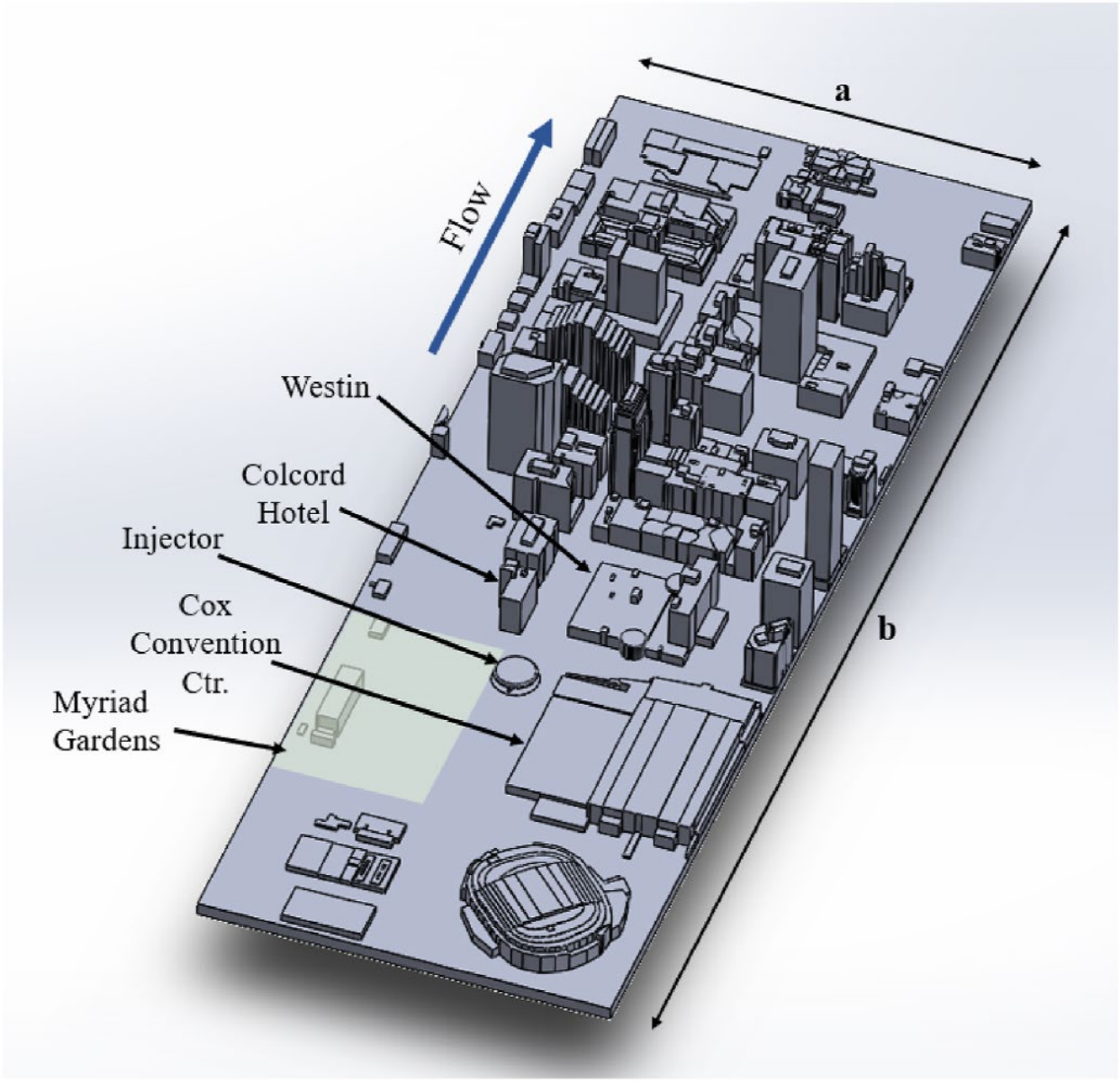

Figure. 1. 1:2206 scaled model of the central business district of Oklahoma City, circa 2003. Main flow direction from South to North is shown. Model length (*b*) is 567 mm, and width (*a*) is 196 mm. (from Homan et al. 2021)

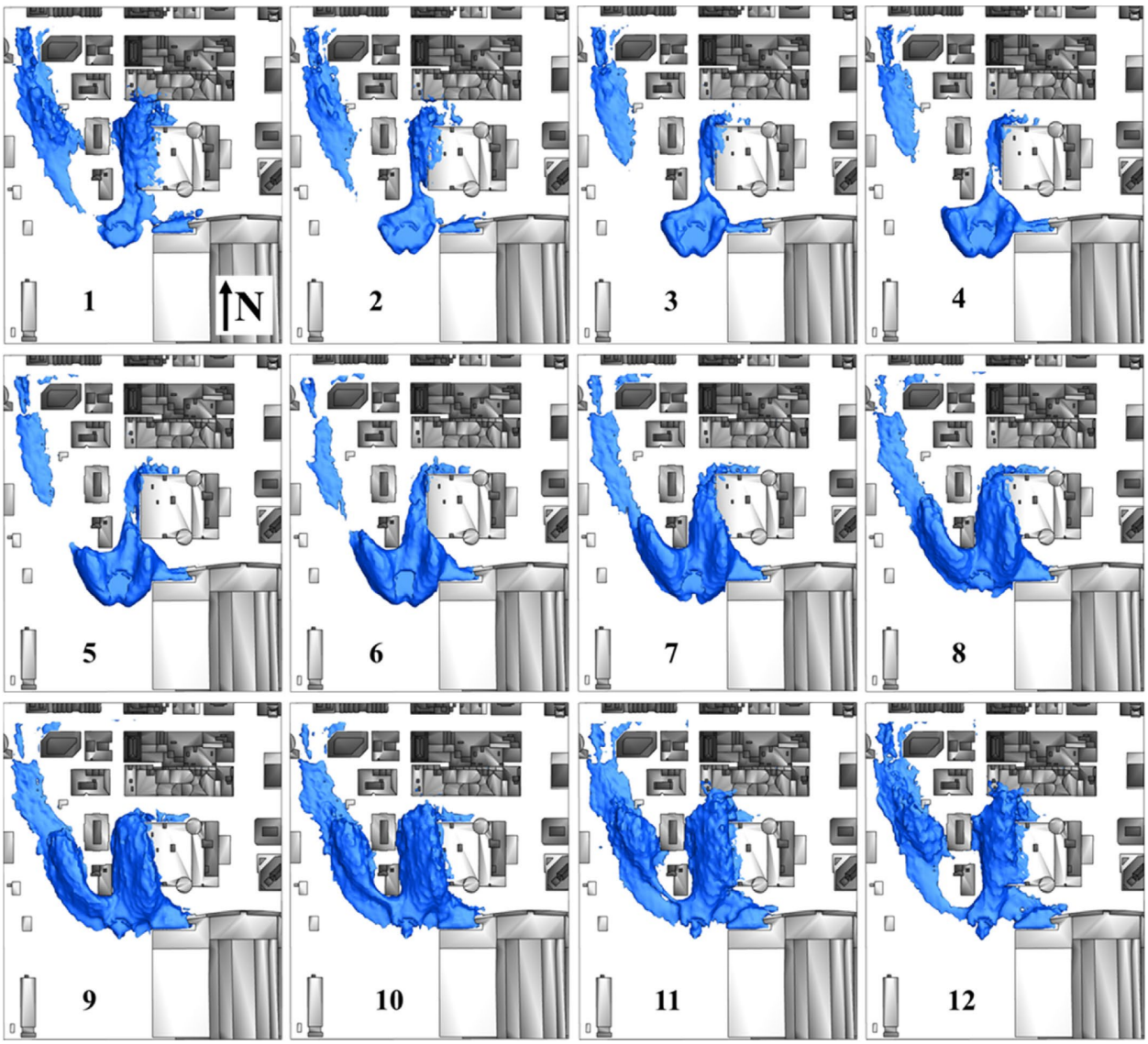

Figure. 2. Top view of isosurfaces at 8% concentration for each of the 12 phases illustrating how the scalar plume interacts with the buildings as it advects downstream. (from Homan et al. 2021)

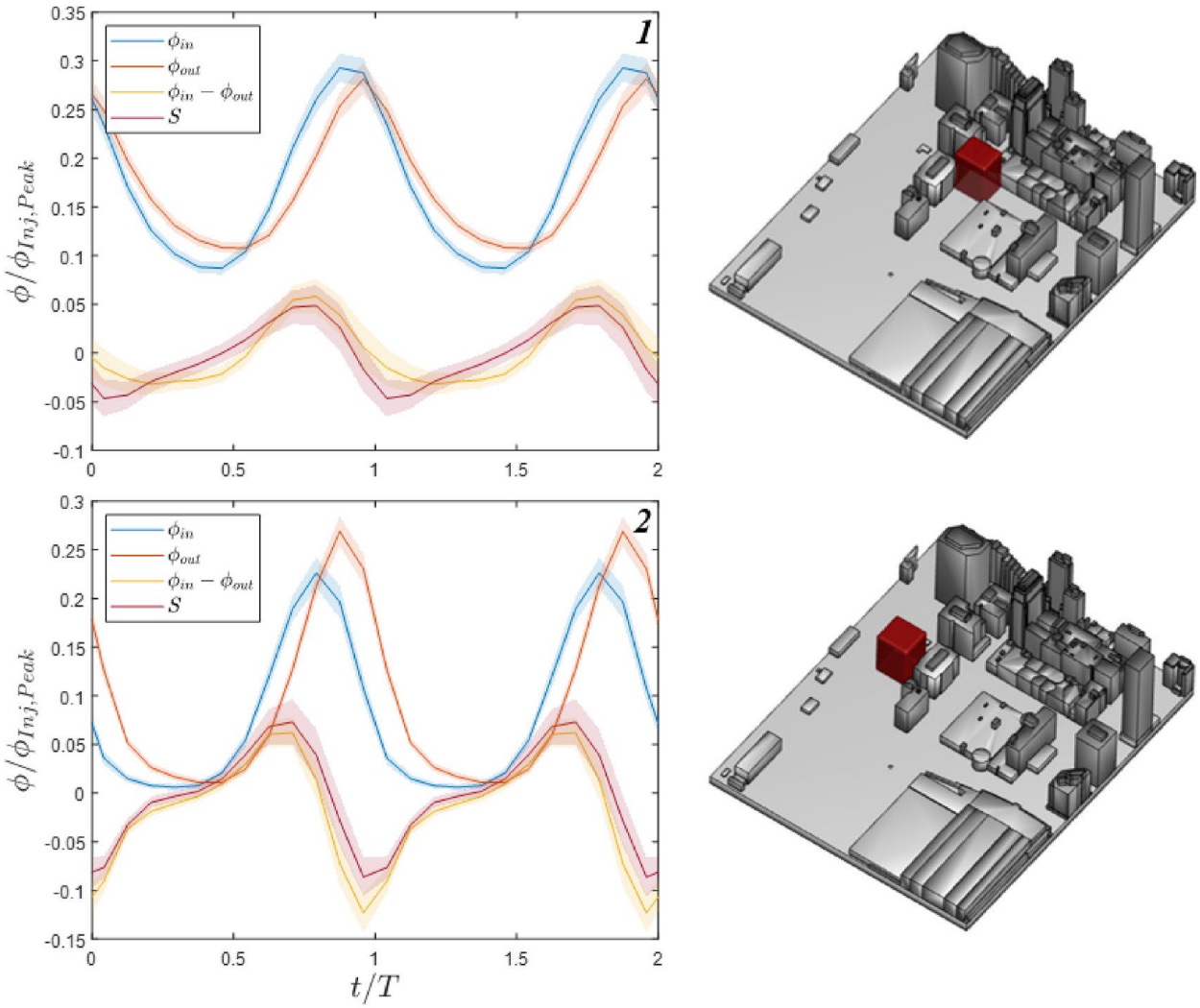

Figure. 3. Advective scalar flux (φ) and transient storage (S) time series for the intersection control volume (top) and a control volume on the west side of the test section (bottom). Time (t) is normalized with respect to the injection cycle period (T). Data is normalized by the peak scalar volume flux ($\varphi_{Inj,Peak}$) out of the injector. 95% confidence intervals for the scalar flux curves are represented by the shaded bands. (from Homan et al. 2021)

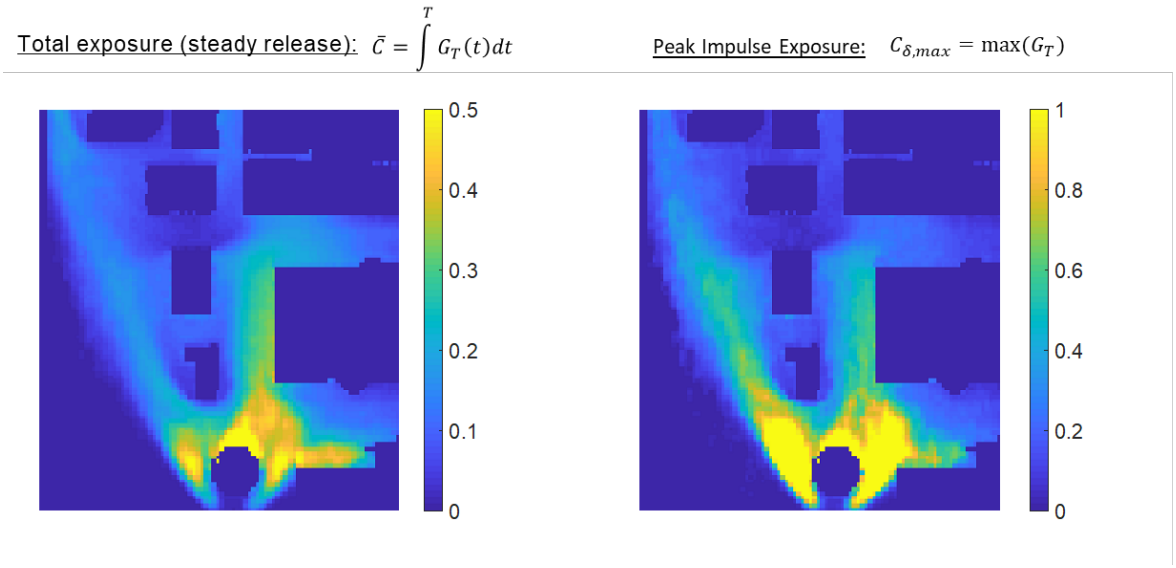

Figure 4. Local total and peak exposure at street level calculated from the DGF.

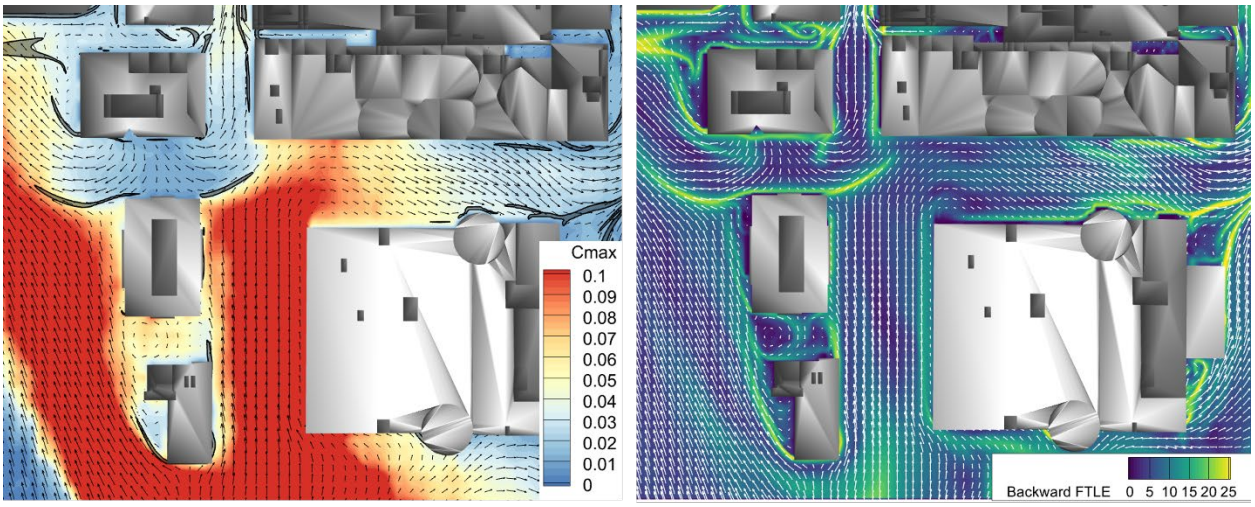

(a) (b)

Figure 5. Impact of mean flow transport boundaries on plume dispersion near ground level. (a) Contours of maximum concentration at each point measured over the transient injection cycle. In-plane mean velocity vectors are also shown. The gray shaded regions indicate transport boundaries extracted from the finite time Lyapunov exponent field. (b) Contours of the backward FTLE field used to define transport boundaries overlaid with in-plane velocity vectors.

Bibliography

Chung, D, Mooradian, L, Rhee, J, Fuhrman, G, Homan, T, Helmer, D, Benson, M, Elkins, C, Banko, A (2020) Three-dimensional concentration and velocity measurements of a pulsatile contaminant release in a model of Oklahoma City, Proc ASME 2020 IMECE, Nov 15-19, 2020, Portland, OR, USA

Homan TA, Benson MJ, Banko, AJ, Elkins CJ, Chung DH, Rhee J, Mooradian LD, Eaton JK, Magnetic resonance imaging measurements of a scalar dispersion for a scaled urban transient release, Building and Environment, 205 (2021) 108163

Klein P, Leitl B, Schatzmann M, Concentration fluctuations in a downtown urban area. Part II: analysis of Joint Urban 2003 wind-tunnel measurements, Environ. Fluid Mech. 11 (2011) 43–60